

Investigating the Accretion Nature of Binary Supermassive Black Hole Candidate SDSS J025214.67-002813.7

ADI FOORD,¹ XIN LIU,^{2,3} KAYHAN GÜLTEKIN,⁴ KEVIN WHITLEY,⁴ FANGZHENG SHI,^{5,6} AND YU-CHING CHEN^{2,3,7}

¹*Kavli Institute of Particle Astrophysics and Cosmology, Stanford University, Stanford, CA 94305, USA*

²*Department of Astronomy, University of Illinois at Urbana-Champaign, Urbana, IL 61801, USA*

³*National Center for Supercomputing Applications, University of Illinois at Urbana-Champaign, Urbana, IL 61801, USA*

⁴*Department of Astronomy and Astrophysics, University of Michigan, Ann Arbor, MI 48109*

⁵*School of Astronomy and Space Science, Nanjing University, Nanjing 210023, China*

⁶*Key Laboratory of Modern Astronomy and Astrophysics, Nanjing University, Nanjing 210023, China*

⁷*Center for AstroPhysical Surveys, National Center for Supercomputing Applications, Urbana, IL, 61801, USA*

ABSTRACT

We present results on a multi-wavelength analysis of SDSS J025214.67-002813.7, a system which has been previously classified as a binary AGN candidate based on periodic signals detected in the optical light curves. We use available radio–X-ray observations of the system to investigate the true accretion nature. Analyzing new observations from *XMM-Newton* and *NuSTAR*, we characterize the X-ray emission and search for evidence of circumbinary accretion. Although the 0.5–10 keV spectrum shows evidence of an additional soft emission component, possibly due to extended emission from hot nuclear gas, we find the spectral shape consistent with a single AGN. Compiling a full multi-wavelength SED, we also search for signs of circumbinary accretion, such as a “notch” in the continuum due to the presence of minidisks. We find that the radio–optical emission agrees with the SED of a standard, radio-quiet, AGN, however there is a large deficit in emission blueward of ~ 1400 Å. Although this deficit in emission can plausibly be attributed to a binary AGN system, we find that the SED of SDSS J0252–0028 is better explained by emission from a reddened, single AGN. However, future studies on the expected hard X-ray emission associated with binary AGN (especially in the unequal-mass regime), will allow for more rigorous analyses of the binary AGN hypothesis.

Keywords: X-ray active galactic nuclei (2035) — Supermassive black holes (1663) — Accretion (14) — Galaxy mergers (608)

1. INTRODUCTION

A binary supermassive black hole (SMBH) represents the final stage of a galaxy merger, where the two massive host galaxies have likely been interacting for hundreds of megayears to gigayears (Begelman et al. 1980). The merging system is classified as a binary when the SMBHs are gravitationally bound in a Keplerian orbit, and for a wide range SMBH masses and host galaxy environments this occurs at orbital separations < 10 pc (Mayer et al. 2007; Dotti et al. 2007; Khan et al. 2012). The fate and final coalescence of the system strongly depends on the amount of matter the SMBHs can interact with (Sesana et al. 2007; Merritt et al. 2007). As the last stage before coalescence, binary SMBHs represent an observable link between galaxy mergers and gravitational wave events. They are strong emitters of low-frequency gravitational waves, which are expected to dominate the gravitational

wave background signal detected by pulsar timing arrays (PTAs; Burke-Spolaor et al. 2019), and they are direct precursors to gravitational-wave events detectable by future space-based laser interferometers (Sesana et al. 2007).

Currently, detections of binary SMBHs are limited to systems where both black holes are actively accreting (active galactic nuclei, or AGN) and emitting light across the electromagnetic spectrum. Given the small physical separations between the two SMBHs, the angular resolution afforded by radio interferometry is required to spatially resolve binary AGN systems, such as in the serendipitous discovery of 0402+379 (Rodriguez et al. 2006). However, radio detections of binary AGN remain limited to relatively low-redshifts (where separations below 1 pc can only be probed up to $z = 0.1$) and systems with two radio-bright AGN (where only $\sim 15\%$

of AGN are expected to be radio loud; see, e.g., Hooper et al. 1995; Kellermann et al. 2016). On top of this, blind surveys with the VLBI networks are limited by the narrow (\sim arcsec-scale) fields of view. As a result, the number of confirmed binary AGN remains small.

Given the difficulty associated with directly detecting binary AGN, many indirect detection techniques are used to search for the elusive systems. One of the most popular methods is to identify quasars with photometric variability, and in particular, periodic signals in their light curves. Periodicity in light curves may arise from various reasons, such as jet precession (where the presence of a companion can introduce a periodicity in the velocity of an otherwise straight jet; see Hardee et al. 1994; Deane et al. 2014), the dynamics of a secondary periodically intercepting the primary SMBH’s accretion disk (i.e., OJ 287; see Valtonen et al. 2008 and the recent review in Dey et al. 2019), or accretion via a circumbinary disk (Hayasaki et al. 2007; MacFadyen & Milosavljević 2008; Roedig et al. 2012, 2014; D’Orazio et al. 2013; Farris et al. 2014). Recently, systematic scans of large areas of the sky carried out via time domain surveys allow for statistical searches for periodic variability in large samples of quasars (Valtonen et al. 2008; Graham et al. 2015; Charisi et al. 2016; Li et al. 2016; Liu et al. 2019; Bon et al. 2016; Chen et al. 2020). Such analyses are complicated by the fact that AGN light curves are characterized by stochastic, red noise variability; it has been shown that this red noise can be misidentified as a periodic signal with time baselines fewer than 5 periods (Vaughan et al. 2016). Although these surveys have collectively found over 100 binary AGN candidates, to date there are no confirmed binary AGN with separations at the sub-milliparsec scale.

A different approach is to use available multi-wavelength observations to search for evidence of circumbinary accretion (see, e.g., Foord et al. 2017). Circumbinary accretion is expected at small separations (when the typical accretion disk size is larger than the binary separation a ; Milosavljević & Phinney 2005). Here, two accretion disks around each supermassive black hole (“mini-disks”) are surrounded by a larger, circumbinary accretion disk. The mini-disks extend to a tidal truncation radius (i.e., where the tidal torques of the disks balance the viscous torque of the circumbinary accretion disk), where values are less than $a/2$ (Paczynski 1977, but see Roedig et al. 2014 for how the radius depends on the mass ratio of the system). In later stages, the angular momentum of material falling from the circumbinary accretion disk may exceed that of the inner-most stable orbits (ISCO) of the SMBHs, and material will fall directly into each SMBH (see Gültekin & Miller 2012;

Tanaka & Haiman 2013; Gold et al. 2014; Roedig et al. 2014). Each accretion scenario will manifest differently in the spectral energy distribution (SED) of a binary AGN, where dips in the optical – UV bands or very little high-energy emission is observed (see Roedig et al. 2014; Foord et al. 2017). Complications to these simple scenarios naturally arise when accounting for stream shock-ing, or when supersonic material from the circumbinary accretion disk hits the outer edge of the mini disks. The high-energy signal associated with these types of events can wash out any dip in the optical regime of the SED (Roedig et al. 2014; Farris et al. 2015a,b). This is especially true for systems where the dips in emission are expected to be subtle with respect to the overall shape of the SED (which depend on the mass ratio between the secondary and primary SMBH and the accretion rates of each SMBH see Section 3 for more details).

Here we present a multi-wavelength analysis of binary AGN candidate SDSS J025214.67–002813.7 (hereafter SDSS J0252–0028), located at $z = 1.53$. It has an estimated virial black hole mass of $M = 10^{8.4 \pm 0.1} M_{\odot}$, physical separation on the order of ≈ 4 miliparsecs (or 200 Schwarzschild radii), and a binary mass ratio on the order of ~ 0.1 (Liao et al. 2021). SDSS J0252–0028 was part of a large systematic search for periodic light curves in 625 quasars via combining Dark Energy Survey Supernova (DES-SN) Y6 observations with archival SDSS-S82 data (Chen et al. 2020). Briefly, quasars were flagged as having significant periodicity in their light curves if (1) at least two photometric bands had a 3σ detection of the same periodicity in the periodogram analysis, (2) the detected periodicity was the dominant signal with respect to the background (red noise) and (3) the same periodicity was also identified in the autocorrelation function (ACF) analysis (see Liao et al. 2021 for more details). Among the 5 quasars flagged as significant periodic candidates, SDSS J0252–0028 was the most significant detection based on ~ 4.6 cycles detected over a 20 year-long baseline. Recent X-ray observations via *XMM-Newton* and *NuSTAR*, along with available radio (VLA), mid-IR (*WISE*), near-IR (UKIDSS), optical (SDSS), and UV (*GALEX*) observations, allow for a multi-wavelength analysis to search for evidence of two supermassive black holes.

Our paper is organized in the following manner: in Section 2 we analyze new X-ray observation of SDSS J0252–0028 and evaluate the 0.5–10 keV spectrum for evidence of a binary AGN system; in Section 3 we present the multi-wavelength SED and compare the emission to both single and binary AGN emission models; in Section 4 we discuss our results and test for effects of reddening; and in Section 5 we review our conclusions.

We assume a standard Λ CDM cosmology of $\Omega_\Lambda = 0.7$, $\Omega_M = 0.3$, and $H_0 = 70 \text{ km s}^{-1} \text{ Mpc}^{-1}$.

2. X-RAY OBSERVATIONS

SDSS J0252-0028 was targeted by *NuSTAR* and *XMM-Newton* in a joint *NuSTAR* Cycle 6 Proposal (PI: Liu, ID: 6061). The quasar was observed for 100 ks and 50 ks with *NuSTAR* and *XMM-Newton* on 2020-08-30 (observation ID 60601009002) and 2020-08-02 UT (observation ID 0870810201). The *NuSTAR* exposure time was set to achieve at least ~ 10 counts under the assumption of a typical optical quasar SED. The *XMM-Newton* exposure time was set to achieve ~ 200 counts for a $\sim 10\%$ flux measurement and a simultaneous fit to the X-ray spectral index within ± 0.3 and the intrinsic hydrogen column density to an upper limit of $\sim 10^{21} \text{ cm}^{-2}$ (both at $\sim 90\%$ confidence).

All errors evaluated in the following section are done at the 95% confidence level and error bars quoted in the following section are calculated with Monte Carlo Markov Chains via the XSPEC tool `chain`.

2.1. *NuSTAR*

We follow the standard process *nupipeline* embedded in the software package NuSTARDAS v1.9.2 to clean the event file of *NuSTAR* observation. We find no emission consistent with an X-ray point source within $100''$ of the SDSS-listed optical center of SDSS J0252-0028. We calculate a 3σ upper limit for 3–10 keV and 10–79 keV flux of $8.8 \times 10^{-14} \text{ erg s}^{-1}$ and $67 \times 10^{-14} \text{ erg s}^{-1}$, respectively, within a circular region with radius of $100''$ centered on the optical center.

2.2. *XMM-Newton*

We clean and process the *XMM-Newton* EPIC pn observation using the *XMM-Newton* Science Analysis System (SAS) software package v18.0.0. The quasar's net count rate and flux value are determined using XSPEC, version 12.11.1 (Arnaud 1996). We generate the event list with the standard pipeline *epproc*. We filtered the event list from high-background time intervals and calculate a good exposure time of 42.59 ks. The quasar was identified as an X-ray point source coincident with the nominal, SDSS-listed optical center of SDSS J0252-0028. Counts are extracted from a circular region with radius of $32''$ centered on the X-ray source center, using a source-free circular region with radius of $90''$ for the background extraction. The spectrum was rebinned via the `specgroup` tool to ensure a minimum signal-to-noise ratio of 2 over the 0.3–10 keV band.

To characterize the X-ray emission, and search for evidence of two accreting supermassive black holes, we fit

the observed-frame 0.5–10 keV spectrum with 3 different models: Model 1: an absorbed red-shifted power-law (`phabs` \times `zphabs` \times `zpow`), and Models 2 and 3: an absorbed red-shifted broken power-law (`phabs` \times `zphabs` \times `zbnkpow`, where the photon index values are tied for Model 2). We expect that Model 1 and Model 2 should return results consistent with one-another, however comparing Model 2 and Model 3 allow us to test for the presence of two AGN, which may be contributing X-ray emission from individual accretion disks (and thus, two power-law photon indices may better describe the X-ray emission).

We implement the Cash statistic (`cstat`; Cash 1979) to best assess the quality of our model fits. In particular, we quantify whether Model 3 is preferred over Model 2 by evaluating whether there is a statistically significant improvement in the fit, such that $\Delta C_{\text{stat}} > \Delta N_{\text{fp}} \times 2.71$ (where ΔN_{fp} represents the difference in number of free parameters between the models; Tozzi et al. 2006; Brightman & Ueda 2012), corresponding to a fit improvement with 90% confidence (Brightman et al. 2014). *K*-corrections are not applied to the *XMM-Newton* data, as we directly measure the flux density from the spectrum. As expected, we find that Model 1 and Model 2 return consistent results; but using the ΔC_{stat} criterion stated above, we find that Model 3 results in a significant improvement in the fit compared to Model 2. However, the best-fit values for the power-law photon indices Γ_1 and Γ_2 are unconstrained and pegged to values consistent with the low ($\Gamma_1 \approx 1$) and high ($\Gamma_2 \approx 3$) end of the allowed range (where values less than 1 or greater than 3 are usually considered non-physical; see Ishibashi & Courvoisier 2010). These results may reflect that the X-ray spectrum is consistent with emission from a single AGN, but requires additional components to a simple power-law.

Thus, we add several additional components to the absorbed power-law to test if they better describe the X-ray emission. In particular, we look at a partially covered power-law (`phabs` \times (`zphabs` \times `zpow`) $+$ `zpow`), where the photon indices of each power-law are tied; Model 4) and a power-law with diffuse gas to account for possible extended soft X-ray emission in the nucleus (`phabs` \times (`zphabs` \times `zpow`) $+$ `APEC`), with abundance fixed at solar value; Model 5). We find that the best-fit parameters from Model 4 are consistent with Model 1, where partially absorbed power-law component does not result in a better fit (which is expected, given low-levels of the extragalactic hydrogen column density, N_H , found across all spectral models; see Table 1). Model 5 results in a significantly improved fit compared to Model 1, meeting our ΔC_{stat} criterion. However, similar to

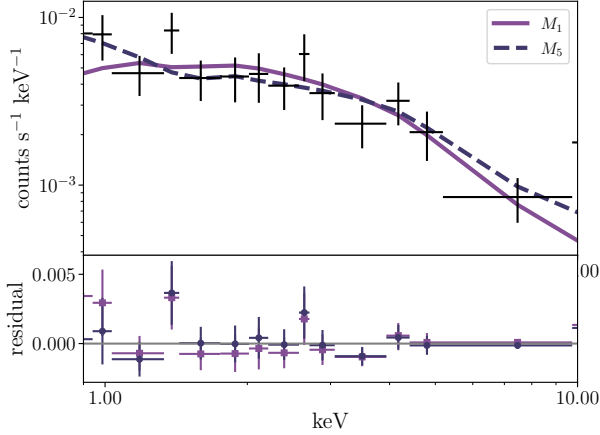


Figure 1. The rest-frame *XMM-Newton* spectrum for SDSS J0252–0028 (*top*). The spectrum has been rebinned via the `specgroup` tool to ensure a minimum signal-to-noise ratio of 2 over observed-frame 0.3–10 keV band. We show best-fits for both Model 1 (an absorbed red-shifted power-law – `phabs` × `zphabs` × `zpow`) and Model 5 (a power-law with diffuse gas – `phabs` × `((zphabs × zpow) + APEC)`). Although Model 5 results in a significantly improved fit compared to Model 1, the posteriors returned by `chain` show that the preferred value for the power-law photon index Γ is non-physical. An additional soft emission component may be present within the region of extracted counts, such as extended soft X-rays from hot nuclear gas. Given the non-physical value for Γ returned by Model 5, we accordingly assume the simple absorbed power-law fit as our best model (Model 1). We measure a 0.5 – 10 keV flux of $9.1^{+3.1}_{-3.9} \times 10^{-13}$ erg s $^{-1}$, corresponding to a 2 – 10 keV luminosity of $6.1^{+1.4}_{-2.0} \times 10^{44}$ erg s $^{-1}$ at $z=1.53$.

Model 3, the posteriors returned by `chain` show that the preferred value for the power-law photon index Γ is non-physical and pegged at 1. Evaluating the spectral fits (see Fig. 1), an additional soft emission component may be present within the region of extracted counts, possibly due to extended soft X-rays from hot nuclear gas. However, given the non-physical value for Γ returned by Model 5, we accordingly assume the simple absorbed power-law fit as our best model (Model 1). We measure a 0.5–10 keV flux of $9.1^{+3.1}_{-3.9} \times 10^{-13}$ erg s $^{-1}$, corresponding to a 2–10 keV luminosity of $6.1^{+1.4}_{-2.0} \times 10^{44}$ erg s $^{-1}$ at $z = 1.53$. In Figure 1 we show the X-ray spectrum of SDSS J0252–0028, along with the fits from Model 1 and Model 5. We list the best-fit values for model parameters in Table 1.

3. MULTI-WAVELENGTH SED

In the following section, we construct a multi-wavelength SED of SDSS J0252–0028 (see also Liao et al. 2021, where this data set is first presented). Similar to the analysis presented in Foord et al. (2017), we combine all available multi-wavelength observations, and compare the SED to the standard non-blazar AGN

Table 1. *XMM-Newton* Spectral Fits

Model	N_H	Γ_1	Γ_2	kT	N_{fp}	C_{stat}
(1)	(2)	(3)	(4)	(5)	(6)	(7)
1	$< 10^{-2}$	$1.5^{+1.0}_{-0.5}$	3	41.4
2	$< 10^{-2}$	$1.5^{+0.8}_{-0.5}$	$1.5^{+0.8}_{-0.5}$...	4	41.4
3	$< 10^{-2}$	$1.1^{+1.8}_{-0.1}$	$2.8^{+0.2}_{-1.7}$...	5	37.1
4	$< 10^{-2}$	$1.5^{+0.8}_{-0.4}$	$1.5^{+0.8}_{-0.4}$...	4	41.4
5	$< 10^{-2}$	$1^{+1.9}_{-0}$...	$1.2^{+8.8}_{-0.5}$	5	35.6

Note. – Columns: (1) Model number, where Model 1 is an absorbed red-shifted power-law (`phabs` × `zphabs` × `zpow`), Model 2 and 3 are an absorbed red-shifted broken power-law (`phabs` × `zphabs` × `zbknpow`, where the photon index values are tied for Model 2), Model 4 is a partially covered power-law (`phabs` × `(zphabs × zpow) + zpow`), and Model 5 is a power-law with diffuse gas (`phabs` × `(zphabs × zpow) + APEC`); (2) the best-fit extragalactic column density in units of 10^{22} cm $^{-2}$; (3) the best-fit spectral index for Γ_1 ; (4) the best-fit spectral index for Γ_2 (only relevant for Model 3); (5) best-fit spectral value for kT (only relevant for Model 5); (6) the number of free parameters for a given model; (7) the Cash statistic for the best-fit. Error bars represent the 95% confidence level of each distribution.

SEDs presented in Shang et al. (2011). To correct for the effective narrowing of the filter width with redshift, we adopt the K -correction relation as presented in Richards et al. (2006). In particular, the $K(z)$ relation for power-law continuum is given by $K = -2.5(1 + \alpha_\nu) \log(1 + z)$, assuming $F_\nu \propto \nu^{-\alpha_\nu}$.

The available SED observations include a radio flux measurement from the Karl G. Jansky Very Large Array (VLA; Thompson et al. 1980), where the rest-frame 6 GHz luminosity is measured in Chen et al. (2021); archival MIR photometry from the Wide-field Infrared Survey Explorer (*WISE*, Wright et al. 2010); archival NIR photometry from the UKIRT Infrared Deep Sky Survey (UKIDSS, Lawrence et al. 2007); archival optical photometry from the Sloan Digital Sky Survey (SDSS, York et al. 2000); and archival UV photometry from the Galaxy Evolution Explorer (*GALEX*, Martin et al. 2005). We correct the archival MIR–UV magnitudes for extinction using dust maps from Schlafly & Finkbeiner (2011) and reddening curves from Fitzpatrick (1999). K -corrections are then applied assuming values of $\alpha = -1.0, -0.5, -1.57$, for the IR, optical, and UV measurements (Shang et al. 2011; Ivezić et al. 2002; Richards et al. 2006). We also include our X-ray observations from *XMM-Newton* (Jansen et al. 2001), and *NuSTAR* (Harrison et al. 2013). The luminosities for each rest-frame frequency are listed in Table 2.

Table 2. Multi-wavelength Luminosity Values

Filter/Detector	Telescope/Survey	$\log \nu$	$\log \nu L_\nu$
(1)	(2)	(3)	(4)
C-band	VLA	9.78	39.98 ± 0.63
W4	<i>WISE</i>	13.5	< 45.76
W3	<i>WISE</i>	13.8	< 45.28
W2	<i>WISE</i>	14.2	44.99 ± 0.11
W1	<i>WISE</i>	14.4	44.96 ± 0.24
J	UKIDSS	14.5	45.21 ± 0.05
K	UKIDSS	14.7	45.16 ± 0.06
H	UKIDSS	14.8	44.94 ± 0.07
<i>z</i>	SDSS	14.93	45.17 ± 0.14
<i>i</i>	SDSS	15.00	45.34 ± 0.39
<i>r</i>	SDSS	15.01	45.35 ± 0.23
<i>g</i>	SDSS	15.21	45.36 ± 0.24
<i>u</i>	SDSS	15.32	45.45 ± 0.31
NUV	<i>GALEX</i>	15.52	44.12 ± 0.45
FUV	<i>GALEX</i>	15.69	< 43.50
EPIC pn	<i>XMM-Newton</i>	18.16	$44.79^{+0.55}_{-0.50}$
...	<i>NuSTAR</i>	19.04	< 46.02

Note. – Columns: (1) Filter or detector; (2) Telescope or survey; (3) rest-frame frequency assuming a redshift of $z = 1.53$, in units of hertz. The *XMM-Newton* and *NuSTAR* frequency corresponds to the central rest-frame frequency of their respective observing ranges (i.e., 6 and 45 keV); (4) extinction- and K -corrected luminosity assuming a luminosity distance $D_L = 11.36$ Gpc, in units of erg s^{-1} . Please see Section 3 for details on extinction values and K -corrections applied.

In Figure 2 we plot the full multi-wavelength SED of SDSS J0252–0028 where, following the normalization procedure in Shang et al. 2011, the flux density of our data is normalized to $\lambda \approx 4200$ Å. This value is estimated by interpolating between our bluest UKIDSS data point, at rest-frame $\lambda \approx 4934$ Å, and our reddest SDSS data point, at rest-frame $\lambda \approx 3530$ Å. A simple comparison between the data and the Shang et al. (2011) SED shows a good agreement between the emission of SDSS J0252–0028 and that of a radio-quiet AGN. However, there is a clear deficit of emission from SDSS J0252–0028 between the NIR and UV frequencies, with a large drop in emission near 1400 Å. Furthermore, given the FUV *GALEX* upper-limit at rest-frame ~ 600 Å, it is possible that the slope of the drop is larger than presented in Figure 2.

3.1. Comparison to binary AGN accretion models

This drop in emission in the SED may be a result a binary AGN accretion mode. In particular, if SDSS

J0252–0028 is a binary AGN system with separation $a = 200 R_S$ (where $R_S = 2GMc^{-2}$ is the Schwarzschild radius for a black hole with mass M), as estimated in Liao et al. (2021), the binary is well into the gravitational-wave dominated regime. Here, circumbinary accretion is likely and we may expect that individual accretion disks have formed around each SMBH. In such a scenario, any radiation that a standard accretion disk would radiate between the inner edge of the circumbinary disk and the tidal truncation radii of the minidisks will be missing. This missing emission can produce a notch in the thermal continuum spectrum (e.g., Gültekin & Miller 2012; Kocevski et al. 2012; Roedig et al. 2012; Tanaka et al. 2012; Tanaka & Haiman 2013; Roedig et al. 2014, and see Farris et al. 2015b for simulations where notches become obscured).

Following a similar procedure as outlined in Foord et al. (2017), we use the analytical calculations derived in Roedig et al. (2014) to analyze how the SED shape is affected by the presence of a notch. In particular, we model the specific luminosity integrated from the circumbinary disk and the two minidisks assuming that the primary and secondary BHs are accreting at rates $\dot{M}_{pri} = f_{pri}\dot{M}$ and $\dot{M}_{sec} = f_{sec}\dot{M}$. Here, \dot{M}_{pri} and \dot{M}_{sec} are the mass accretion rates of the primary and secondary, and \dot{M} is the circumbinary accretion rate. These calculations assume that the circumbinary disk is in inflow equilibrium, such that $f_{pri} + f_{sec} = 1$. Values of f_{pri} and f_{sec} depend on the mass ratio of the system, q , and simulations have shown that for most values of mass ratio, $f_{sec} > f_{pri}$ (but as q increases towards equal mass, the accretion rate ratio goes to unity, see Farris et al. 2014).

Hydrodynamical simulations of circumbinary accretion disks around binary SMBHs with a range of mass ratios ($0.026 < q < 1.0$) have shown that significant periodicity in the accretion rates occurs only at $q > 0.1$ (Farris et al. 2014). At these mass ratios, the binary torques are strong enough to lead to periodicity in the accretion rates, and thus the light curve of the system. Previously, the light curves of SDSS J0252–0028 were modeled with both $q = 0.11$ and $q = 0.43$ (two mass ratio regimes probed by Farris et al. 2014); however, the fits to the data did not strongly prefer one model over the other, and a value of $q = 0.11$ was adopted to interpret the results (Liao et al. 2021).

In Figure 2 we show two examples of SED models with notches for both $q = 0.11$ and $q = 0.43$. Here, we adopt the predicted f_{pri} and f_{sec} values expected for each mass ratio as estimated in Farris et al. (2014). As evident, as the mass ratio decreases and the secondary’s accretion rate dominates, the notch occurs at

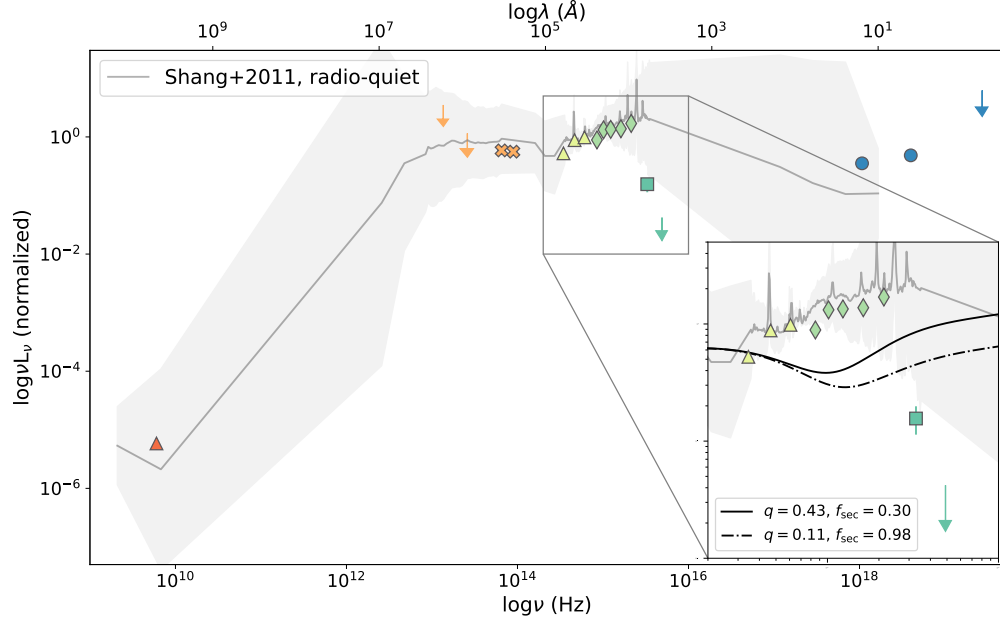


Figure 2. The rest-frame multi-wavelength spectral energy density of SDSS J0252–0028. We plot the radio flux density upper limit from VLASS (red pentagon), MIR photometry from *WISE* (orange “x” markers for the W2 and W1 filter detections, and upper-limits for the W3 and W4 filters), NIR photometry from UKIDSS (yellow triangles), optical photometry from SDSS (green diamonds), UV photometry from *GALEX* (dark green square for the NUV detection, and upper limit for the FUV), and X-ray photometry from *XMM-Newton* (dark blue circles) and *NuSTAR* (upper limit). In gray we overplot the composite non-blazar radio-quiet quasar SED from Shang et al. (2011). In general we find a good agreement between the SED of SDSS J0252–0028 and that of the composite quasar SED. However, SDSS J0252–0028 appears to have a deficit of emission between the NIR and FUV bands, significantly dropping off near ~ 1400 Å. In the inset we show various models for a possible “notch” in the accretion disk of a binary AGN, with different mass ratios (q) and accretion rates for the primary, f_{pri} , and secondary, f_{sec} (where $f_{pri} + f_{sec} = 1$, see Section 3.1 for more detail). Although lower values of q and higher values f_{sec} will result in deeper and wider notch, we find that the most extreme values fail to accurately capture the FUV *GALEX* upper-limit.

shorter wavelengths and deepens; this is a result of the primary SMBH’s accretion flow barely contributing to the total SED (Roedig et al. 2014). Because we don’t expect significant modulation in the accretion rates at $q < 0.1$, our mass ratio model of $q = 0.11$ represents the lowest and deepest notch expected for this system. We find that this model is unable to match the shape of SDSS J0252–0028’s SED, and in particular predicts a lower level of emission between rest-frame 1400–3500 Å (SDSS) and a higher level of emission at $\lambda < 1400$ Å (*GALEX*) than observed.

Lastly, disregarding the mass ratio constraint of $q > 0.1$ for significant accretion modulation, extremely low (high) values of q (f_{sec}) can further deepen the notch to potentially match the *GALEX* data points. However the size of the notch will also widen – resulting in larger differences between the predicted and observed rest-frame optical and NUV emission (UKIDSS and SDSS observations, see Figure 2).

3.1.1. Enhanced Hard X-ray Emission

Many computational results on binary mergers indicate that binary SMBHs should have enhanced hard X-ray emission relative to a single SMBH (Roedig et al. 2014; Farris et al. 2015b; Ryan & MacFadyen 2017; Tang et al. 2018; d’Ascoli et al. 2018), a result of supersonic streams from the circumbinary disk shocking at the minidisk edges. Yet, results from these simulations have a wide range in the predicted energy at which these enhancements should occur, from tens of keV up to over 100 keV. Although Roedig et al. (2014) predict a Wien-like spectrum may adequately describe the emission, the large range of possible peak temperatures does not allow us to carry out an in-depth analysis of a possible hot-spot X-ray contribution to the multi-wavelength SED.

However, using the derivations presented in Roedig et al. (2014), we can estimate an approximate peak temperature of an additional Wien-like spectrum by calculating the post-shock temperature, T_{ps} , which is proportional to the binary’s semimajor axis, a , and mass ratio, q : $T_{ps} \propto (a/50R_S)^{-1} \times (1 + q^{0.7})^{-1}$ (see

Roedig et al. 2014 for more details). We consider possible temperatures for the stream-shocking emission from SDSS J0252-0028, given an assumed semimajor axis $a = 200 R_S$ and a range of q values between 0.1–1.0. Adopting the assumption presented in Roedig et al. 2014 that a mass ratio $q = 1.0$ and semimajor axis $a = 50 R_S$ will result in an additional Wien-like spectrum with peak energy 100 keV, we estimate that excess emission from hot spots in SDSS J0252-0028 could peak between rest-frame 25–42 keV, or observed-frame 10–16 keV. Although our *XMM-Newton* falls below this energy window, the spectrum shows no evidence of excess hard X-ray emission with respect to an absorbed power-law model. Furthermore, our *NuSTAR* upper-limit does not allow us to measure for the presence of enhanced hard X-ray emission at higher energies. Additional studies on the hard X-ray emission associated with binary AGN (especially in the unequal-mass regime), will allow for more rigorous hard X-ray analyses on binary AGN candidates in the future.

Lastly, we note that the enhanced X-ray emission expected from binary AGN raises the possibility of binaries having different X-ray spectral indices (see Section 2 for our analysis on the X-ray spectrum) or optical to X-ray spectral indices (α_{ox} , see, e.g., Yuan et al. 1998; Vignali et al. 2003; Strateva et al. 2005; Steffen et al. 2006; Just et al. 2007; Kelly et al. 2008; Lusso et al. 2010) than single AGN. This ratio is defined as $\alpha_{\text{ox}} = -\log [L_{2 \text{ keV}}/L_{2500}]/2.605$, and has been measured to strongly correlate with the optical luminosity of the AGN at 2500 Å (e.g., Silverman et al. 2005; Lusso et al. 2010). We estimate the approximate rest-frame 2500 Å flux density using the available SDSS r band photometry (which corresponds to rest-frame emission at ≈ 2440 Å), and we use the *XMM-Newton* fit results from Model 1 (see Section 2) to estimate the 2 keV flux density. We calculate an $\alpha_{\text{ox}} \approx 1.6$, consistent within the error of the range expected from single AGN with similar 2500 Å luminosities (see Lusso et al. 2010).

4. POSSIBLE EFFECTS OF REDDENING

In the following section we discuss alternative physical explanations for the observed multi-wavelength SED of SDSS J0252-0028, which is not well explained by either a standard AGN or a binary AGN system. In particular, we investigate whether the effects of reddening can match the steep drop off seen near ~ 1400 Å.

The unusual SED of SDSS J0252-0028, with infrared and optical emission typical of an AGN but strongly cut off through the near UV, is similar (albeit less extreme) to the SED of contentious binary AGN candidate Mrk 231 (see Smith et al. 1995; Veilleux et al. 2013; Leighly

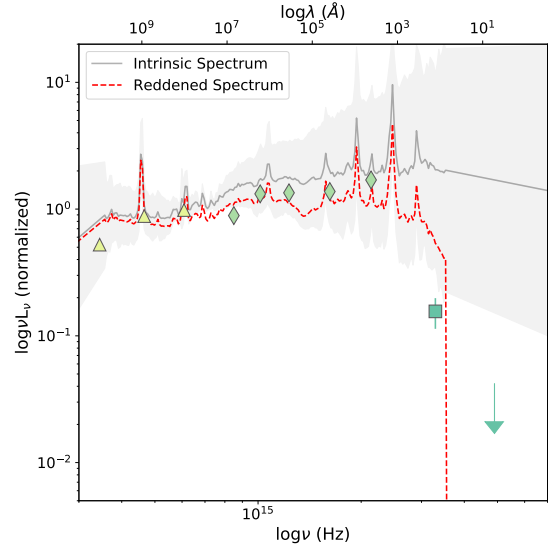


Figure 3. The best-fit reddened spectrum (red dashed line) when fitting the composite radio-quiet SED from Shang et al. (2011) (gray line) to the photometric data points of SDSS J0252-0028 (between rest-frame 87300 Å and 610 Å). We plot NIR photometry from UKIDSS (yellow triangles), optical photometry from SDSS (green diamonds), and UV photometry from *GALEX* (dark green square for the NUV detection, and upper limit for the FUV). We apply the reddening law from Fitzpatrick (1999), although we find consistent results when using reddening law presented in Goobar (2008) (which has been used in past analyses of binary AGN candidate Mrk 231). We find best-fit values of $A_V = 0.17$ and $R(V) = 2.54$. Overall, once accounting for circumstellar reddening, the composite single quasar spectrum agrees well the measured emission of SDSS J0252-0028.

et al. 2014; Yan et al. 2015; Leighly et al. 2016). The binary AGN hypothesis proposed for Mrk 231 is that the smaller-mass black hole accretes as a thin disk, dominating the weak UV emission, while the larger-mass black hole radiates inefficiently as an Advection Dominated Accretion Flow (ADAF), and both are surrounded by a circumbinary disk (dominating the optical and IR emission). Here, emission blueward of the near UV is dominated by accretion onto the smaller mass black hole and thus the SED is expected to have a steep drop-off toward the UV, near the inner edge of the circumbinary disk (Yan et al. 2015). However, it has been shown that the unusual shape is consistent with circumstellar reddening (Leighly et al. 2014), and that if the observed FUV continuum is intrinsic, it fails by a factor of 100 in powering the observed strength of the near-infrared emission lines (Leighly et al. 2016).

Following the logic presented in Leighly et al. (2014), we apply a reddening correction from Fitzpatrick (1999)

to the composite radio-quiet quasar SED from [Shang et al. \(2011\)](#) to fit the photometric data points of SDSS J0252–0028 between rest-frame 87300 Å and 610 Å (i.e., the *WISE*, UKIDSS, SDSS, and *GALEX* data points). We fit for the best values of A_V and $R(V)$ via the `python` non-linear least-squares fitting package `lmfit`. In addition to the reddening relation presented in [Fitzpatrick \(1999\)](#), we also use the analytical correction presented in [Goobar \(2008\)](#), which assumes a spherical scattering medium (and used by [Leighly et al. 2014](#) when analyzing Mrk 231). Although this reddening law is typically used to describe low values of $R(V)$ around Type Ia supernovae, a spherical geometry with significant optical depth (and multiple scatterings) allows for the removal of more blue photons from the line of sight than a screen.

The best-fit results of both reddening laws are consistent within the errors, although the reddening correction from [Fitzpatrick \(1999\)](#) yields a slightly better fit (as determined from the Bayesian information criterion values). We find best-fit values of $A_V = 0.17$ and $R(V) = 2.54$. In Figure 3 we plot the results of our best-fit reddened quasar SED along with the photometric data points from the SED of SDSS J0252–0028. With the addition of circumstellar reddening, the composite quasar spectrum agrees well with the measured emission of SDSS J0252–0028. The best-fit $R(V)$ value is indicative of dust similar to that in the Milky Way (where $R(V) \sim 3.1$).

Although we find the SED of SDSS J0252–0028 best described by a single AGN obscured by circumstellar dust, it is possible that the system is a binary where a notch has been masked by (i) circumstellar dust, (ii) the tail-end of a Wien-like spectrum that peaks at hard (>10 keV) energies, or (iii) a combination of both. Follow-up spectroscopy in the IR, which is relatively free of the effects of reddening, can help disentangle whether circumstellar reddening is acting on its own. For example, [Leighly et al. \(2016\)](#) analyze observed He I ($\lambda = 10830$ Å), P β ($\lambda = 12818$ Å), P α ($\lambda = 18751$ Å), and C IV ($\lambda = 1549$ Å) emission lines of Mrk 231 with *Cloudy* to show that the measured equivalent widths and emission-line ratios in the IR are not reproducible with the binary AGN model proposed by [Yan et al. \(2015\)](#).

5. CONCLUSIONS

In this work we present a multi-wavelength analysis of binary AGN candidate SDSS J0252–0028. SDSS J0252–0028 was part of a large systematic search for long-term periodic light curves in 625 quasars, and was flagged as a binary AGN candidate based on a significant periodicity measured in 20 year SDSS–DES data ([Chen et al. 2020](#); [Liao et al. 2021](#)). New X-ray observations

via *XMM-Newton* and *NuSTAR*, along with available radio (VLA), mid-IR (*WISE*), near-IR (UKIDSS), optical (SDSS), and UV (*GALEX*) observations, have been combined to search for evidence of two accreting supermassive black holes. The main results and implications of this work can be summarized as follows.

1. We analyze new X-ray observations of SDSS J0252–0028 (obtained by *NuSTAR* and *XMM-Newton*). We find no emission consistent with an X-ray point source within $100''$ of the SDSS-listed optical center of SDSS J0252–0028 when analyzing the *NuSTAR* data. We calculate a 3σ upper limit for 3–10 keV and 10–79 keV flux of 8.8×10^{-14} erg s $^{-1}$ and 67×10^{-14} erg s $^{-1}$, respectively. We identified the quasar as an X-ray point source in the *XMM-Newton*, and search for evidence of two accreting supermassive black holes by fitting the observed-frame 0.5–10 keV spectrum with 5 different models. Although an additional soft emission component may be present within the region of extracted counts, a simple absorbed power-law remains the best-fit model, as expected from a single AGN. We measure a 0.5–10 keV flux of $9.1^{+3.1}_{-3.9} \times 10^{-13}$ erg s $^{-1}$, corresponding to a 2–10 keV luminosity of $6.1^{+1.4}_{-2.0} \times 10^{44}$ erg s $^{-1}$ at $z = 1.53$.
2. We combine all available multi-wavelength observations and compare the SED to a standard non-blazar AGN SED. The available SED observations include a radio flux measurement from the VLA, MIR photometry from *WISE*, NIR photometry from UKIDSS, optical photometry from SDSS, and UV photometry from *GALEX*. We find a good agreement between the SED of SDSS J0252–0028 and that of a standard AGN; however there is a clear deficit of emission from SDSS J0252–0028 between the optical and UV frequencies, with a large drop in emission near rest-frame 1400 Å.
3. We investigate whether the drop in emission in the SED may be a result of circumbinary accretion, where individual disks have formed around each SMBH. Using analytical calculations derived in [Roedig et al. \(2014\)](#), we analyze how the SED of a standard quasar could be affected by the presence of a notch. However, even at the most extreme values of mass ratios and accretion rates, we find the model is unable to match the shape of SDSS J0252–0028’s SED.
4. We estimate an approximate peak temperature of an additional Wien-like spectrum in the hard X-rays, as a result of possible stream shocking in a

binary AGN system. We find that excess emission from hot spots in SDSS J0252–0028 could peak between rest-frame 25–42 keV, or observed-frame 10–16 keV. Although our *XMM-Newton* falls below this energy window, the spectrum shows no evidence of excess hard X-ray emission with respect to an absorbed power-law model. Furthermore, our *NuSTAR* upper-limit does not allow us to measure for the presence of enhanced hard X-ray emission at higher energies. We search for other evidence of enhanced X-ray emission by analyzing α_{OX} , and calculate a value of 1.6, consistent within the error of the range expected from a single AGN.

5. We investigate whether the effects of circumstellar reddening can match the steep drop-off in the multi-wavelength SED near 1400 Å. Following the logic presented in Leighly et al. (2014), we apply a reddening correction from Fitzpatrick (1999) to a standard non-blazar AGN SED to fit the photometric data points of SDSS J0252–0028 between rest-frame 87300 Å and 610 Å. With the addition of circumstellar reddening, the standard quasar spectrum agrees well with the measured emission of SDSS J0252–0028. We find best-fit values of $A_V = 0.17$ and $R(V) = 2.54$.

We have shown through various analyses that there is an absence of evidence supporting SDSS J0252–0028 as a binary AGN system. However, given the small number of currently confirmed binary AGN, the best method to distinguish a binary AGN from a single AGN is consistently changing. These studies are further complicated by the fact that analyses searching for signs of circumbinary accretion will likely be dependent on the unique parameters of a given binary AGN system. For SDSS J0252–0028, future observations of IR emission lines can be used to better understand whether a binary AGN accretion model is able to power the emission seen at longer wavelengths. Overall, hard X-ray emission signatures may be the most telling sign of circumbinary accretion—however, current results from simulations are extremely model-dependent (with a wide range of predicted energies where enhancements should occur). A more rigorous analysis of the binary AGN hypothesis for SDSS J0252–0028 can be made with future studies on the expected hard X-ray emission associated with binary AGN (especially in the unequal-mass regime).

knowledge support by NSF grant AST-2108162 and NASA grant 80NSSC21K0060. YCC acknowledges support by the government scholarship to study aboard from the ministry of education of Taiwan and the Illinois Survey Science Graduate Student Fellowship. *NuSTAR* is a project led by the California Institute of Technology (Caltech), managed by the Jet Propulsion Laboratory (JPL), and funded by the National Aeronautics and Space Administration (NASA). We thank the *NuSTAR* Operations, Software and Calibrations teams for support with these observations. This research has made use of the *NuSTAR* Data Analysis Software (NuSTAR-DAS) jointly developed by the ASI Science Data Center (ASDC, Italy) and the California Institute of Technology (Caltech, USA). This work is also based on observations obtained with *XMM-Newton*, an ESA science mission with instruments and contributions directly funded by ESA Member States and NASA. This work makes use of data obtained as part of the Karl G. Jansky Very Large Array (VLA), UKIRT Infrared Deep Sky Survey (UKIDSS), Wide-field Infrared Survey (*WISE*), Sloan Digital Sky Survey (SDSS), and the Galaxy Evolution Explorer (*GALEX*). The National Radio Astronomy Observatory is a facility of the National Science Foundation operated under cooperative agreement by Associated Universities, Inc. UKIDSS and *WISE* are joint projects of the University of California, Los Angeles, and the Jet Propulsion Laboratory/California Institute of Technology, funded by the National Aeronautics and Space Administration. Funding for the Sloan Digital Sky Survey has been provided by the Alfred P. Sloan Foundation, the U.S. Department of Energy Office of Science, and the Participating Institutions. *GALEX* is a NASA Small Explorer, launched in 2003 April. We acknowledge NASA’s support for construction, operation, and science analysis for the *GALEX* mission, developed in cooperation with the Centre National d’Etudes Spatiales of France and the Korean Ministry of Science and Technology. Lastly, this research has made use of NASA’s Astrophysics Data System.

Facilities: *NuSTAR* - The NuSTAR (Nuclear Spectroscopic Telescope Array) mission, *XMM-Newton* X-Ray Multimirror Mission satellite, VLA, *WISE*, UKIDSS, SDSS, *GALEX*

Software: NuSTARDAS, SAS, XSPEC,

AF acknowledges support by the Porat Postdoctoral Fellowship at Stanford University. XL and YCC ac-

REFERENCES

- Arnaud, K. A. 1996, in *Astronomical Society of the Pacific Conference Series*, Vol. 101, *Astronomical Data Analysis Software and Systems V*, ed. G. H. Jacoby & J. Barnes, 17
- Begelman, M. C., Blandford, R. D., & Rees, M. J. 1980, *Nature*, 287, 307, doi: [10.1038/287307a0](https://doi.org/10.1038/287307a0)
- Bon, E., Zucker, S., Netzer, H., et al. 2016, *The Astrophysical Journal Supplement Series*, 225, 29, doi: [10.3847/0067-0049/225/2/29](https://doi.org/10.3847/0067-0049/225/2/29)
- Brightman, M., Nandra, K., Salvato, M., et al. 2014, *MNRAS*, 443, 1999, doi: [10.1093/mnras/stu1175](https://doi.org/10.1093/mnras/stu1175)
- Brightman, M., & Ueda, Y. 2012, *MNRAS*, 423, 702, doi: [10.1111/j.1365-2966.2012.20908.x](https://doi.org/10.1111/j.1365-2966.2012.20908.x)
- Burke-Spolaor, S., Taylor, S. R., Charisi, M., et al. 2019, *A&A Rv*, 27, 5, doi: [10.1007/s00159-019-0115-7](https://doi.org/10.1007/s00159-019-0115-7)
- Cash, W. 1979, *ApJ*, 228, 939, doi: [10.1086/156922](https://doi.org/10.1086/156922)
- Charisi, M., Bartos, I., Haiman, Z., et al. 2016, *MNRAS*, 463, 2145, doi: [10.1093/mnras/stw1838](https://doi.org/10.1093/mnras/stw1838)
- Chen, Y.-C., Liu, X., Liao, W.-T., & Guo, H. 2021, *MNRAS*, 507, 4638, doi: [10.1093/mnras/stab2397](https://doi.org/10.1093/mnras/stab2397)
- Chen, Y.-C., Liu, X., Liao, W.-T., et al. 2020, *MNRAS*, 499, 2245, doi: [10.1093/mnras/staa2957](https://doi.org/10.1093/mnras/staa2957)
- d’Ascoli, S., Noble, S. C., Bowen, D. B., et al. 2018, *ApJ*, 865, 140, doi: [10.3847/1538-4357/aad8b4](https://doi.org/10.3847/1538-4357/aad8b4)
- Deane, R. P., Paragi, Z., Jarvis, M. J., et al. 2014, *Nature*, 511, 57, doi: [10.1038/nature13454](https://doi.org/10.1038/nature13454)
- Dey, L., Gopakumar, A., Valtonen, M., et al. 2019, *Universe*, 5, 108, doi: [10.3390/universe5050108](https://doi.org/10.3390/universe5050108)
- D’Orazio, D. J., Haiman, Z., & MacFadyen, A. 2013, *MNRAS*, 436, 2997, doi: [10.1093/mnras/stt1787](https://doi.org/10.1093/mnras/stt1787)
- Dotti, M., Colpi, M., Haardt, F., & Mayer, L. 2007, *MNRAS*, 379, 956, doi: [10.1111/j.1365-2966.2007.12010.x](https://doi.org/10.1111/j.1365-2966.2007.12010.x)
- Farris, B. D., Duffell, P., MacFadyen, A. I., & Haiman, Z. 2014, *ApJ*, 783, 134, doi: [10.1088/0004-637X/783/2/134](https://doi.org/10.1088/0004-637X/783/2/134)
- . 2015a, *MNRAS*, 446, L36, doi: [10.1093/mnrasl/slu160](https://doi.org/10.1093/mnrasl/slu160)
- . 2015b, *MNRAS*, 447, L80, doi: [10.1093/mnrasl/slu184](https://doi.org/10.1093/mnrasl/slu184)
- Fitzpatrick, E. L. 1999, *PASP*, 111, 63, doi: [10.1086/316293](https://doi.org/10.1086/316293)
- Foord, A., Gültekin, K., Reynolds, M., et al. 2017, *ApJ*, 851, 106, doi: [10.3847/1538-4357/aa9a39](https://doi.org/10.3847/1538-4357/aa9a39)
- Gold, R., Paschalidis, V., Etienne, Z. B., Shapiro, S. L., & Pfeiffer, H. P. 2014, *PhRvD*, 89, 064060, doi: [10.1103/PhysRevD.89.064060](https://doi.org/10.1103/PhysRevD.89.064060)
- Goobar, A. 2008, *ApJL*, 686, L103, doi: [10.1086/593060](https://doi.org/10.1086/593060)
- Graham, M. J., Djorgovski, S. G., Stern, D., et al. 2015, *Nature*, 518, 74, doi: [10.1038/nature14143](https://doi.org/10.1038/nature14143)
- Gültekin, K., & Miller, J. M. 2012, *ApJ*, 761, 90, doi: [10.1088/0004-637X/761/2/90](https://doi.org/10.1088/0004-637X/761/2/90)
- Hardee, P. E., Cooper, M. A., & Clarke, D. A. 1994, *ApJ*, 424, 126, doi: [10.1086/173877](https://doi.org/10.1086/173877)
- Harrison, F. A., Craig, W. W., Christensen, F. E., et al. 2013, *ApJ*, 770, 103, doi: [10.1088/0004-637X/770/2/103](https://doi.org/10.1088/0004-637X/770/2/103)
- Hayasaki, K., Mineshige, S., & Sudou, H. 2007, *PASJ*, 59, 427, doi: [10.1093/pasj/59.2.427](https://doi.org/10.1093/pasj/59.2.427)
- Hooper, E. J., Impey, C. D., Foltz, C. B., & Hewett, P. C. 1995, *ApJ*, 445, 62, doi: [10.1086/175673](https://doi.org/10.1086/175673)
- Ishibashi, W., & Courvoisier, T. J.-L. 2010, *A&A*, 512, A58, doi: [10.1051/0004-6361/200913587](https://doi.org/10.1051/0004-6361/200913587)
- Ivezić, Ž., Menou, K., Knapp, G. R., et al. 2002, *AJ*, 124, 2364, doi: [10.1086/344069](https://doi.org/10.1086/344069)
- Jansen, F., Lumb, D., Altieri, B., et al. 2001, *A&A*, 365, L1, doi: [10.1051/0004-6361:20000036](https://doi.org/10.1051/0004-6361:20000036)
- Just, D. W., Brandt, W. N., Shemmer, O., et al. 2007, *ApJ*, 665, 1004, doi: [10.1086/519990](https://doi.org/10.1086/519990)
- Kellermann, K. I., Condon, J. J., Kimball, A. E., Perley, R. A., & Ivezić, Ž. 2016, *ApJ*, 831, 168, doi: [10.3847/0004-637X/831/2/168](https://doi.org/10.3847/0004-637X/831/2/168)
- Kelly, B. C., Bechtold, J., Trump, J. R., Vestergaard, M., & Siemiginowska, A. 2008, *ApJS*, 176, 355, doi: [10.1086/533440](https://doi.org/10.1086/533440)
- Khan, F. M., Berentzen, I., Berczik, P., et al. 2012, *ApJ*, 756, 30, doi: [10.1088/0004-637X/756/1/30](https://doi.org/10.1088/0004-637X/756/1/30)
- Kocevski, D. D., Faber, S. M., Mozena, M., et al. 2012, *ApJ*, 744, 148, doi: [10.1088/0004-637X/744/2/148](https://doi.org/10.1088/0004-637X/744/2/148)
- Lawrence, A., Warren, S. J., Almaini, O., et al. 2007, *MNRAS*, 379, 1599, doi: [10.1111/j.1365-2966.2007.12040.x](https://doi.org/10.1111/j.1365-2966.2007.12040.x)
- Leighly, K. M., Terndrup, D. M., Baron, E., et al. 2014, *ApJ*, 788, 123, doi: [10.1088/0004-637X/788/2/123](https://doi.org/10.1088/0004-637X/788/2/123)
- Leighly, K. M., Terndrup, D. M., Gallagher, S. C., & Lucy, A. B. 2016, *ApJ*, 829, 4, doi: [10.3847/0004-637X/829/1/4](https://doi.org/10.3847/0004-637X/829/1/4)
- Li, Y.-R., Wang, J.-M., Ho, L. C., et al. 2016, *ApJ*, 822, 4, doi: [10.3847/0004-637X/822/1/4](https://doi.org/10.3847/0004-637X/822/1/4)
- Liao, W.-T., Chen, Y.-C., Liu, X., et al. 2021, *MNRAS*, 500, 4025, doi: [10.1093/mnras/staa3055](https://doi.org/10.1093/mnras/staa3055)
- Liu, X., Hou, M., Li, Z., et al. 2019, *ApJ*, 887, 90, doi: [10.3847/1538-4357/ab54c3](https://doi.org/10.3847/1538-4357/ab54c3)
- Lusso, E., Comastri, A., Vignali, C., et al. 2010, *A&A*, 512, A34, doi: [10.1051/0004-6361/200913298](https://doi.org/10.1051/0004-6361/200913298)
- MacFadyen, A. I., & Milosavljević, M. 2008, *ApJ*, 672, 83, doi: [10.1086/523869](https://doi.org/10.1086/523869)
- Martin, D. C., Fanston, J., Schiminovich, D., et al. 2005, *ApJL*, 619, L1, doi: [10.1086/426387](https://doi.org/10.1086/426387)
- Mayer, L., Kazantzidis, S., Madau, P., et al. 2007, *Science*, 316, 1874, doi: [10.1126/science.1141858](https://doi.org/10.1126/science.1141858)
- Merritt, D., Mikkola, S., & Szell, A. 2007, *ApJ*, 671, 53, doi: [10.1086/522691](https://doi.org/10.1086/522691)
- Milosavljević, M., & Phinney, E. S. 2005, *ApJL*, 622, L93, doi: [10.1086/429618](https://doi.org/10.1086/429618)

- Paczynski, B. 1977, *ApJ*, 216, 822, doi: [10.1086/155526](https://doi.org/10.1086/155526)
- Richards, G. T., Strauss, M. A., Fan, X., et al. 2006, *AJ*, 131, 2766, doi: [10.1086/503559](https://doi.org/10.1086/503559)
- Rodriguez, C., Taylor, G. B., Zavala, R. T., et al. 2006, *ApJ*, 646, 49, doi: [10.1086/504825](https://doi.org/10.1086/504825)
- Roedig, C., Krolik, J. H., & Miller, M. C. 2014, *ApJ*, 785, 115, doi: [10.1088/0004-637X/785/2/115](https://doi.org/10.1088/0004-637X/785/2/115)
- Roedig, C., Sesana, A., Dotti, M., et al. 2012, *A&A*, 545, A127, doi: [10.1051/0004-6361/201219986](https://doi.org/10.1051/0004-6361/201219986)
- Ryan, G., & MacFadyen, A. 2017, *ApJ*, 835, 199, doi: [10.3847/1538-4357/835/2/199](https://doi.org/10.3847/1538-4357/835/2/199)
- Schlafly, E. F., & Finkbeiner, D. P. 2011, *ApJ*, 737, 103, doi: [10.1088/0004-637X/737/2/103](https://doi.org/10.1088/0004-637X/737/2/103)
- Sesana, A., Haardt, F., & Madau, P. 2007, *ApJ*, 660, 546, doi: [10.1086/513016](https://doi.org/10.1086/513016)
- Shang, Z., Brotherton, M. S., Wills, B. J., et al. 2011, *ApJS*, 196, 2, doi: [10.1088/0067-0049/196/1/2](https://doi.org/10.1088/0067-0049/196/1/2)
- Silverman, J. D., Green, P. J., Barkhouse, W. A., et al. 2005, *ApJ*, 618, 123, doi: [10.1086/425895](https://doi.org/10.1086/425895)
- Smith, P. S., Schmidt, G. D., Allen, R. G., & Angel, J. R. P. 1995, *ApJ*, 444, 146, doi: [10.1086/175589](https://doi.org/10.1086/175589)
- Steffen, A. T., Strateva, I., Brandt, W. N., et al. 2006, *AJ*, 131, 2826, doi: [10.1086/503627](https://doi.org/10.1086/503627)
- Strateva, I. V., Brandt, W. N., Schneider, D. P., Vanden Berk, D. G., & Vignali, C. 2005, *AJ*, 130, 387, doi: [10.1086/431247](https://doi.org/10.1086/431247)
- Tanaka, T., Menou, K., & Haiman, Z. 2012, *Monthly Notices of the Royal Astronomical Society*, 420, 705
- Tanaka, T. L., & Haiman, Z. 2013, *Classical and Quantum Gravity*, 30, 224012, doi: [10.1088/0264-9381/30/22/224012](https://doi.org/10.1088/0264-9381/30/22/224012)
- Tang, Y., Haiman, Z., & MacFadyen, A. 2018, *MNRAS*, 476, 2249, doi: [10.1093/mnras/sty423](https://doi.org/10.1093/mnras/sty423)
- Thompson, A. R., Clark, B. G., Wade, C. M., & Napier, P. J. 1980, *ApJS*, 44, 151, doi: [10.1086/190688](https://doi.org/10.1086/190688)
- Tozzi, P., Gilli, R., Mainieri, V., et al. 2006, *A&A*, 451, 457, doi: [10.1051/0004-6361:20042592](https://doi.org/10.1051/0004-6361:20042592)
- Valtonen, M. J., Lehto, H. J., Nilsson, K., et al. 2008, *Nature*, 452, 851, doi: [10.1038/nature06896](https://doi.org/10.1038/nature06896)
- Vaughan, S., Uttley, P., Markowitz, A. G., et al. 2016, *MNRAS*, 461, 3145, doi: [10.1093/mnras/stw1412](https://doi.org/10.1093/mnras/stw1412)
- Veilleux, S., Trippe, M., Hamann, F., et al. 2013, *ApJ*, 764, 15, doi: [10.1088/0004-637X/764/1/15](https://doi.org/10.1088/0004-637X/764/1/15)
- Vignali, C., Brandt, W. N., & Schneider, D. P. 2003, *AJ*, 125, 433, doi: [10.1086/345973](https://doi.org/10.1086/345973)
- Wright, E. L., Eisenhardt, P. R. M., Mainzer, A. K., et al. 2010, *AJ*, 140, 1868, doi: [10.1088/0004-6256/140/6/1868](https://doi.org/10.1088/0004-6256/140/6/1868)
- Yan, C.-S., Lu, Y., Dai, X., & Yu, Q. 2015, *ApJ*, 809, 117, doi: [10.1088/0004-637X/809/2/117](https://doi.org/10.1088/0004-637X/809/2/117)
- York, D. G., Adelman, J., Anderson, John E., J., et al. 2000, *AJ*, 120, 1579, doi: [10.1086/301513](https://doi.org/10.1086/301513)
- Yuan, W., Siebert, J., & Brinkmann, W. 1998, *A&A*, 334, 498. <https://arxiv.org/abs/astro-ph/9805118>